Redox Biology 59 (2023) 102552

Contents lists available at ScienceDirect

Redox Biology

journal homepage: www.elsevier.com/locate/redox

Design and characterization of a heterobifunctional degrader of KEAP1

Hao Chen [a,b], Nghi H. Nguyen [a,b], Charlene M. Magtoto [a,b], Simon A. Cobbold [a,b], Grace M. Bidgood [a,b], Lizeth G. Meza Guzman [a,b], Lachlan W. Richardson [a,b], Jason Corbin [b], Amanda E. Au [a,b], Bernhard C. Lechtenberg [a,b], Rebecca Feltham [a,b], Kate D. Sutherland [a,b], Christoph Grohmann [a,b], Sandra E. Nicholson [a,b], Brad E. Sleebs [a,b,*]

[a] The Walter and Eliza Hall Institute of Medical Research, Parkville, 3052, Australia
[b] Department of Medical Biology, The University of Melbourne, Parkville, 3010, Australia

ARTICLE INFO

Keywords:
PROTAC
KEAP1-NRF2 pathway
Antioxidant
ROS
Oxidative stress

ABSTRACT

The Kelch-like ECH-associated protein 1 (KEAP1) - nuclear factor erythroid 2-related factor 2 (NRF2) signaling pathway senses reactive oxygen species and regulates cellular oxidative stress. Inhibiting KEAP1 to activate the NRF2 antioxidant response has been proposed as a promising strategy to treat chronic diseases caused by oxidative stress. Here, we developed a proteolysis targeting chimera (PROTAC) that depletes KEAP1 from cells through the ubiquitin-proteasome pathway. A previously developed KEAP1 inhibitor and thalidomide were incorporated in the heterobifunctional design of the PROTAC as ligands for KEAP1 and CRBN recruitment, respectively. Optimization of the chemical composition and linker length resulted in PROTAC **14** which exhibited potent KEAP1 degradation with low nanomolar DC_{50} in HEK293T (11 nM) and BEAS-2B (<1 nM) cell lines. Furthermore, PROTAC **14** increased the expression of NRF2 regulated antioxidant proteins and prevented cell death induced by reactive oxygen species. Together, these results established a blueprint for further development of KEAP1-targeted heterobifunctional degraders and will facilitate the study of the biological consequences of KEAP1 removal from cells. This approach represents an alternative therapeutic strategy to existing treatments for diseases caused by oxidative stress.

1. Introduction

Cellular oxidative stress occurs when cells are exposed to excessive reactive oxygen species (ROS) and as a consequence, the cellular redox balance cannot be maintained [1]. Chronic exposure to oxidative stress leads to diverse pathologic conditions such as respiratory, autoimmune, and neurodegenerative disorders [2]. Cells are equipped with a sophisticated antioxidant system to combat and eliminate harmful ROS and maintain redox homeostasis [3]. The Kelch-like ECH-associated protein 1 (KEAP1) - nuclear factor erythroid 2-related factor 2 (NRF2) pathway is the principal cellular mechanism that regulates redox balance [4].

KEAP1 is a cysteine-rich protein that acts as an oxidant sensor and a negative regulator of NRF2 [4]. KEAP1 consists of three functional domains, namely the broad complex, tramtrack and a bric-à-brac (BTB) domain, the intervening region (IVR), and the Kelch domain [5]. The BTB domain is responsible for KEAP1 dimerization and interacts with Cullin3/Rbx1 to form an E3 ligase [6–8]. The IVR domain bridges the BTB and the Kelch domain in the KEAP1 complex, enabling the dimerized Kelch domains to recognize and capture cytosolic NRF2 [9]. The Kelch domain adopts a classic β-propeller structure and in the KEAP1 homodimeric complex, interacts with the high-affinity ETGE or low-affinity DLG motifs in the Neh2 domain of the NRF2 protein [10].

Under basal conditions, NRF2 is sequestered by a homodimer of KEAP1/Cullin3/Rbx1 E3 ligase, resulting in NRF2 polyubiquitination and proteasomal degradation [11]. Under oxidative stress, multiple cysteines in KEAP1 are modified by ROS, leading to a conformational change in KEAP1 which prevents NRF2 binding and ubiquitination. NRF2 then accumulates in the cytosol and translocates into the nucleus. In the nucleus, NRF2 binds to antioxidant response elements (ARE) with other co-factors to initiate antioxidant gene expression [12]. Therefore, inhibiting KEAP1 to activate NRF2 signaling has been proposed as a potential therapeutic avenue to treat chronic disorders caused by oxidative stress [13].

To this extent, several electrophilic small molecules that covalently modify Cys151 in the KEAP1 BTB domain have been clinically

* Corresponding author. The Walter and Eliza Hall Institute of Medical Research, 1G Royal Parade, Parkville, 3052, Victoria, Australia.
E-mail address: sleebs@wehi.edu.au (B.E. Sleebs).

https://doi.org/10.1016/j.redox.2022.102552
Received 28 September 2022; Received in revised form 20 November 2022; Accepted 22 November 2022
Available online 26 November 2022

developed but all displayed adverse off-target effects, probably due to the promiscuous potential of these compounds to react with cysteines on other proteins [14]. To overcome the off-target promiscuity, direct and non-covalent inhibitors of KEAP1-NRF2 interaction have been developed that activate NRF2 signaling both *in vitro* and *in vivo*, but to date, none of them have proceeded to clinical trials [14].

Instead of inhibiting the active site of the target protein, removal of the whole protein from cells is an alternative strategy for therapeutic development [15]. In the past two decades, targeted protein degradation using proteolysis-targeting chimeras (PROTAC) has received great interest from both academic researchers and pharmaceutical industries [16]. PROTACs eliminate their target proteins by harnessing the cellular ubiquitin-proteasome system (UPS). A heterobifunctional PROTAC consists of a ligand that binds to the protein of interest (POI) conjugated to an E3 ligase ligand. The E3 ligase ligand recruits an E3 ligase to mediate the ubiquitination of the POI. The E3 ligase complex then dissociates and the ubiquitinylated POI is subsequently degraded by the proteasome [17].

In this study, we designed and characterized a PROTAC to target KEAP1 for proteasomal degradation. The PROTAC exploits a known non-covalent KEAP1 inhibitor (**1**) which we linked to thalidomide, the ligand for cereblon (CRBN)/Cullin4/Rbx1 E3 ligase. Initially, a series of PROTACs were conceived and synthesized with varying linker lengths to assess their ability to degrade KEAP1. The PROTAC with the optimal linker was then characterized for its ability to degrade KEAP1 in various cell lines and activate an NRF2-mediated antioxidant response in cellular assays.

2. Methods and materials

2.1. Chemistry

Chemistry experimental is included in the supplementary information section.

2.2. Biology

2.2.1. Cell culture conditions

HEK293T, HCA7, A549, and BEAS-2B cell lines were obtained from the ATCC. The HepG2-ARE reporter cell line was purchased from BPSBioscience (BPSBioscience, USA). HEK293T, HCA7, A549 cells were cultured in DMEM medium (Gibco, Invitrogen Corp., USA) with 10% fetal bovine serum (FBS) (Gibco, Invitrogen Corp., USA) and penicillin/streptomycin (Gibco, Invitrogen Corp., USA). BEAS-2B cells were cultured in LHC-9 medium (Gibco, Invitrogen Corp., USA) with penicillin/streptomycin. HepG2-ARE reporter cells were cultured in DMEM medium supplied with 1% non-essential amino acids (Gibco, Invitrogen Corp., USA), 1 mM Na pyruvate (Gibco, Invitrogen Corp., USA), penicillin/streptomycin plus 600 μg/mL of Geneticin (Roche, Switzerland). All cell lines were maintained in a humidified incubator at 37 °C with 10% CO_2.

2.2.2. Expression and purification of recombinant human KEAP1-Kelch domain

BL21(DE3) cells were transformed with a pOPINK plasmid encoding the His-GST-KEAP1 Kelch domain (312–624) and grown in 1 L YT cultures to OD_{600} 0.8 in a shaking incubator at 37 °C. The temperature was reduced to 20 °C for 45 min and KEAP1 expression was induced by the addition of 0.5 mM IPTG (Gold Biotechnology, USA). Cultures were harvested by centrifugation after overnight incubation at 20 °C. For purification, cells were resuspended in high-salt binding buffer (50 mM Tris pH 8.0, 500 mM NaCl, 10% sucrose, 10% glycerol) supplemented with leupeptin, lysozyme, DNaseI, $MgCl_2$, and PMSF and lysed by sonication. Lysates were cleared by centrifugation at 40,000 g for 30 min at 4 °C. Protein purification was initiated by passing supernatant over Ni-NTA His-bind resin (Merck Millipore, USA) in gravity flow columns equilibrated with high-salt binding buffer. Ni-NTA His-bind resin was washed with 3 × 10 mL of high-salt binding buffer, and 1 × 6 mL of high-salt binding buffer supplemented with 10 mM imidazole. The protein was then eluted with high-salt binding buffer supplemented with 300 mM imidazole and further purified by size exclusion chromatography using a HiLoad 16/600 Superdex 200 pg column (Cytiva, USA) in 10 mM HEPES pH 7.9, 100 mM NaCl. Protein samples were concentrated, flash-frozen in liquid nitrogen, and stored at −80 °C.

2.2.3. Homogeneous time resolved fluorescence (HTRF) assay

The HTRF assay was performed in a Greiner white 1536-well plate (Interpath, Australia) with buffer containing 25 mM HEPES, pH 7.4, 100 mM NaCl, 0.005% BSA, 0.1% Tween-20, and 1 mM TECP. In the assay, 0.4 nM GST-KEAP1 Kelch domain, 1.25 nM biotin labeled NRF2 peptide (^{82}QLQLDEETGEFL^{93}) and a serial dilution of test compounds was mixed and incubated at room temperature for 1 h. Thereafter, the HTRF mix (37.5 ng/mL anti-GST terbium (Tb) and 180 ng/mL streptavidin-d2) was added and incubated for 2 h. Signal was measured on a PheraSTAR (BMG LABTECH, Germany) using an HTRF module (excitation: 337 nm; emission 1: 665 nm; emission 2: 620 nm).

2.2.4. Immunoblotting

Sample preparation and immunoblotting were performed as previously reported [18]. Briefly, cells were harvested and lysed followed by electrophoresis using SDS PAGE (Invitrogen and 4–12%). Samples were then transferred to a nitrocellulose membrane (Cytiva, USA) and blocked with 5% skim milk for 1 h at room temperature. Proteins were detected by the following antibodies: anti-KEAP1 (sc-365626), anti-GCLM (sc-55586), and horseradish peroxidase (HRP) conjugated anti-β-actin (sc-47778) purchased from Santa Cruz Biotechnology (Santa Cruz, USA). Anti-CRBN (D8H3S) was purchased from Cell Signaling Technology (Cell Signaling Technology, USA), anti-NQO1 (ab34173) from Abcam (Abcam, USA), and anti–HO–1 (MA1112) was purchased from Invitrogen (Invitrogen, USA). HRP conjugated anti-mouse (NA931) and anti-rabbit (NA934) secondary antibodies were purchased from Amersham (Amersham, USA).

2.2.5. ARE-luciferase activity assay

HepG2-ARE cells were seeded into a 96-well plate at a density of 1 × 10^4 cells/well and incubated overnight. Cells were then treated with the indicated concentration of compounds for 48 h and then lysed. Luciferase activity was measured using the Luciferase Reporter Assay Kit (Promega, USA) and a luminometer (Promega, USA) as previously described [19].

2.2.6. Quantitative RT-PCR

RNA was extracted from BEAS-2B cells using Qiagen RNeasy Plus Kits (Qiagen, Germany) following the manufacturer's instructions. The RNA was reverse transcribed into cDNA using a SuperScript IV kit (Thermo Fisher, USA). Quantitative RT-PCR was performed using SyberGreen (Bioline, Australia) on the QuantStudio 12 K Flex Real-Time PCR System (Thermo Fisher, USA). Relative RNA levels were normalized to the *18S* internal control using the delta-delta-cT statistical method. Primers for RT-PCR are listed in Table S1.

2.2.7. MS proteomics

BEAS-2B cells were treated with DMSO, 0.13 μM of PROTAC **14**, or inhibitor **2** for 48 h. Samples were then harvested and lysed with 5% SDS (in 50 mM TEAB) for label-free proteomics. BCA assay was used to confirm protein concentration and 20 μg of protein per sample was processed via micro S-traps (Protifi) as described by the manufacturer (with the exception that chloroacetamide was used for alkylation) and digested with trypsin/Lys-C. Samples were cleaned using SDB prepacked stage tips (GLSicences) and approximately 100 ng of peptide was injected onto a custom Dionex-PAL nanoflow pump connected to a timsTOF pro (Bruker). Peptides were separated using a 48 min gradient

(solvent A, 0.1% formic acid; solvent B, 99.9% acetonitrile/0.1% formic acid) on a C18 analytical column (IonOpticks, Aurora Elite 15 cm × 75 μm ID, 1.7 μm AUR3-15075C18). Data-independent PASEF acquisition was performed (100–1700 *m/z* scan range, 0.6–1.6 Vs/cm^2, and 100 ms ramp and accumulation time) and library-free searching was performed with DIA-NN (v1.8) using the reviewed *Homo sapiens* uniprot database (UP000005640). MS1 and mass accuracy was set to 15 ppm and the precursor FDR was set at 1%. Protein quantification was performed using the DIA-NN in-built MaxLFQ algorithm (using a TopN = 3). Downstream data processing and analysis was performed using the DEP package in R. Protein abundance in **14** and **2** treatment samples was compared to the DMSO control group. Proteins with more than 1.5-fold change and adjusted *P* value less than 0.01 were considered significant.

2.2.8. Flow cytometric detection of cell viability

BEAS-2B cells were seeded in a 48-well plate at a density of 1.2 × 10^4 cells/well and incubated overnight. Cells were then pre-treated with the indicated concentration of compounds for 24 h, followed by 50 μM *tert*-butyl hydroperoxide (tBHP) treatment, a chemical that can generate ROS rapidly in cells, for another 24 h. Cells were then harvested and stained with 1 μg/mL propidium iodide (PI). Data were acquired using a BD FACSymphony flow cytometer and analyzed using BD FlowJo v10 software. Cells were first gated on FSC-A and SSC-A to exclude debris and then gated on FSC-H and FSC-A to exclude doublets. Viability was assessed as %PI negative cells.

2.2.9. PAMPA membrane permeability assay

This assay was performed by BioDuro-Sundia using the following standard protocol. Working solutions of each compound were prepared from 10 mM stock solution in DMSO diluted to a final concentration of 10 μM in PBS buffer (pH 7.4, 1% DMSO). 1% (w/v) lecithin/dodecane was added to the donor side of the Multi Screen Filter Plate, then 10 μM control or test compound working solution is added. The receiver side of the Multi Screen Filter Plates was filled with PBS buffer containing 1% DMSO. The plates were kept at room temperature for 24 h. Samples were collected from the donor and receiver sides. The donor sides samples were diluted 20-fold with PBS (1% DMSO). All receiver and diluted donor side samples were mixed with ACN/MeOH (1:1, v/v) containing 25 ng/mL terfenadine and 50 ng/mL tolbutamide as internal standards. Samples were vortexed and then centrifuged at 4 °C. An aliquot of the supernatant was transferred to a 0.65 mL tube for LC-MS/MS analysis. The MS detection was performed using a SCIEX API 4000 instrument. Each compound was analyzed by reversed phase HPLC using a Kinetex 2.6μ C18 100 Å column (3.0 mm × 30 mm, Phenomenex). Mobile phase – Solvent A: water with 0.1% formic acid, solvent B: ACN with 0.1% formic acid. Analysis of the compound was determined on the basis of the peak area ratio (compound area to IS area) for the two sides; LogPe = Log (C*-Ln(1-[drug]acceptor/[drug]equilibrium)) where C = VD*VA/((VD + VA)*Area*time) and % Recovery = (Total compound mass in donor and receiver compartments at the end of the incubation/ Initial compound mass in the donor compartment) x 100.

3. Results

3.1. Design and binding affinity of KEAP1 PROTACs

Davies et al. disclosed the KEAP1 inhibitor (**1**, Fig. 1A) bearing a 3-phenylpropanoic acid scaffold. It displayed tight KEAP1 binding and potent induction of the NRF2 antioxidant response both *in vitro* and *in vivo* [20]. We selected this compound as the parental KEAP1 recruitment warhead for our PROTAC design. Instead of using the enantiopure molecule **1**, we employed the racemic version **2** (*R*,*S*-stereochemistry at the 3-position of the propanoic acid) (Fig. 1B), in the design of the KEAP1 targeted PROTAC, due to synthetic tractability. To ensure the feasibility of our approach, we synthesized and evaluated compounds **1** and **2** in a KEAP1-Kelch domain – NRF2 peptide HTRF biochemical assay. As expected, the racemic compound **2** was 2-fold less potent than the enantiopure compound **1** (**1**, IC_{50} 0.037 μM; **2**, IC_{50} 0.077 μM), supporting our decision to utilize the racemic version **2** as the KEAP1 ligand in the design of the PROTAC. The co-crystal structure of compound **1** and the KEAP1-Kelch domain revealed the methoxy group on the 7-position of benzotriazole ring was solvent exposed, suggesting this

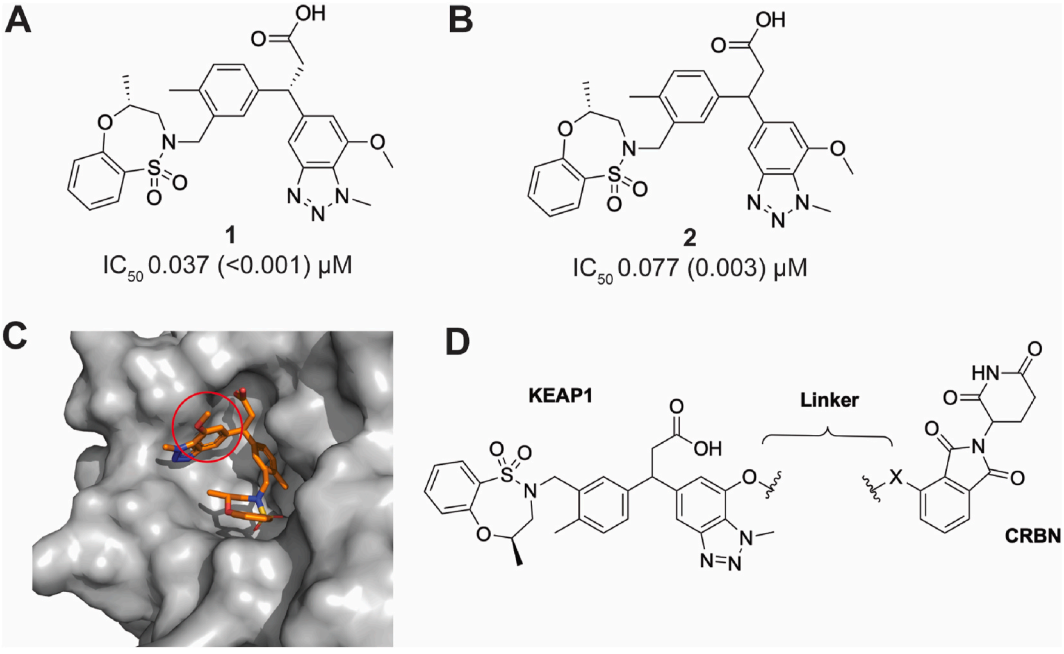

Fig. 1. Design of a CRBN-based KEAP1 degrader. (A) The structure and activity of the KEAP1 inhibitor **1** reported by Davies et al. [20]. (B) Activity of the synthesized racemic KEAP1 inhibitor **2** incorporated in the KEAP1 degrader. (C) KEAP1 inhibitor **1** co-crystalized with the KEAP1-Kelch domain [20]. The red circle highlights the linker attachment site used in the design of a PROTAC. (D) Design and structure of CRBN based KEAP1 degraders used in this study. IC_{50} (SD) values shown represent 3 independent experiments using recombinant KEAP1-Kelch domain in a HTRF biochemical assay. (For interpretation of the references to color in this figure legend, the reader is referred to the Web version of this article.)

would be a suitable position for conjugation of the E3 ligase ligand via a linker (Fig. 1C) [20]. The CRBN E3 ligase has been widely exploited in the development of PROTACs targeting other proteins of interest and its ligands are well characterized [16]. We therefore incorporated thalidomide as the CRBN recruitment ligand in our KEAP1-targeted PROTAC (Fig. 1D).

To synthesize the series of PROTACs bearing different linker lengths and types, intermediate **25** and thalidomide functionalized with a fluoro or carboxylic acid in the 4-position **40**–**41** were employed as key intermediates (Scheme 1). Intermediate **25** was synthesized using a procedure adapted from literature [20,21] starting from phenol **18**. Phenol **18** was alkylated and brominated to give **19** followed by methylation of the amino group and reduction of the nitro group to give the amine **20**. Diazotization of **20** and a Heck reaction gave the cinnamoyl benzotriazole intermediate **22**. Conjugate addition of the boronic acid to **22** gave the aryl derivative **23**, followed by a Mitsunobu reaction, and deprotection of the benzyl ether gave intermediate **25**. Intermediate **25** was then *O*-alkylated with various alkyl halide linkers bearing an azide or Cbz-protected amines to afford **26**, **28**, **30**, **32**, **34**, **36**, and **38**. The azide or Cbz-amine groups were then subjected to hydrogenation conditions to give the corresponding amines **27**, **31**, **33**, **35**, **37**, and **39**. Finally, the thalidomide component was installed via an amide coupling or a SnAr reaction with thalidomide derivatives **40**–**41**, and then the *tert*-butyl group was deprotected to afford the PROTACs **3**–**14**.

The binding affinity of synthesized PROTACs to the KEAP1-Kelch domain was evaluated using the HTRF biochemical assay (Table 1). In general, the attachment of a linker conjugated to a CRBN ligand did not significantly impair the binding affinity of the resulting PROTACs to KEAP1 (0.059–0.15 μM). The exceptions were derivatives **4**, **5**, and **12**, which showed a greater than 3-fold reduction in KEAP1 binding affinity compared to inhibitor **2**. The inhibitory activity against KEAP1 supported our PROTAC design strategy and warranted further characterization of these analogs in cell-based assays to assess KEAP1 degradation.

3.2. KEAP1 degradation by PROTACs in HEK293T cells

The ability of the synthesized PROTACs to degrade KEAP1 was assessed in HEK293T cells. Cells were treated with 1 μM PROTAC for 5 or 24 h, and KEAP1 levels were then analyzed by immunoblotting (Fig. 2A and S1). PROTACs possessing a longer linker length (>7 atoms, **8** to **13**) resulted in a robust reduction in KEAP1 protein levels at both time points compared to PROTACs with shorter linker lengths (**3** to **7**). To study their efficacy in more detail, PROTACs **8** to **13** were evaluated

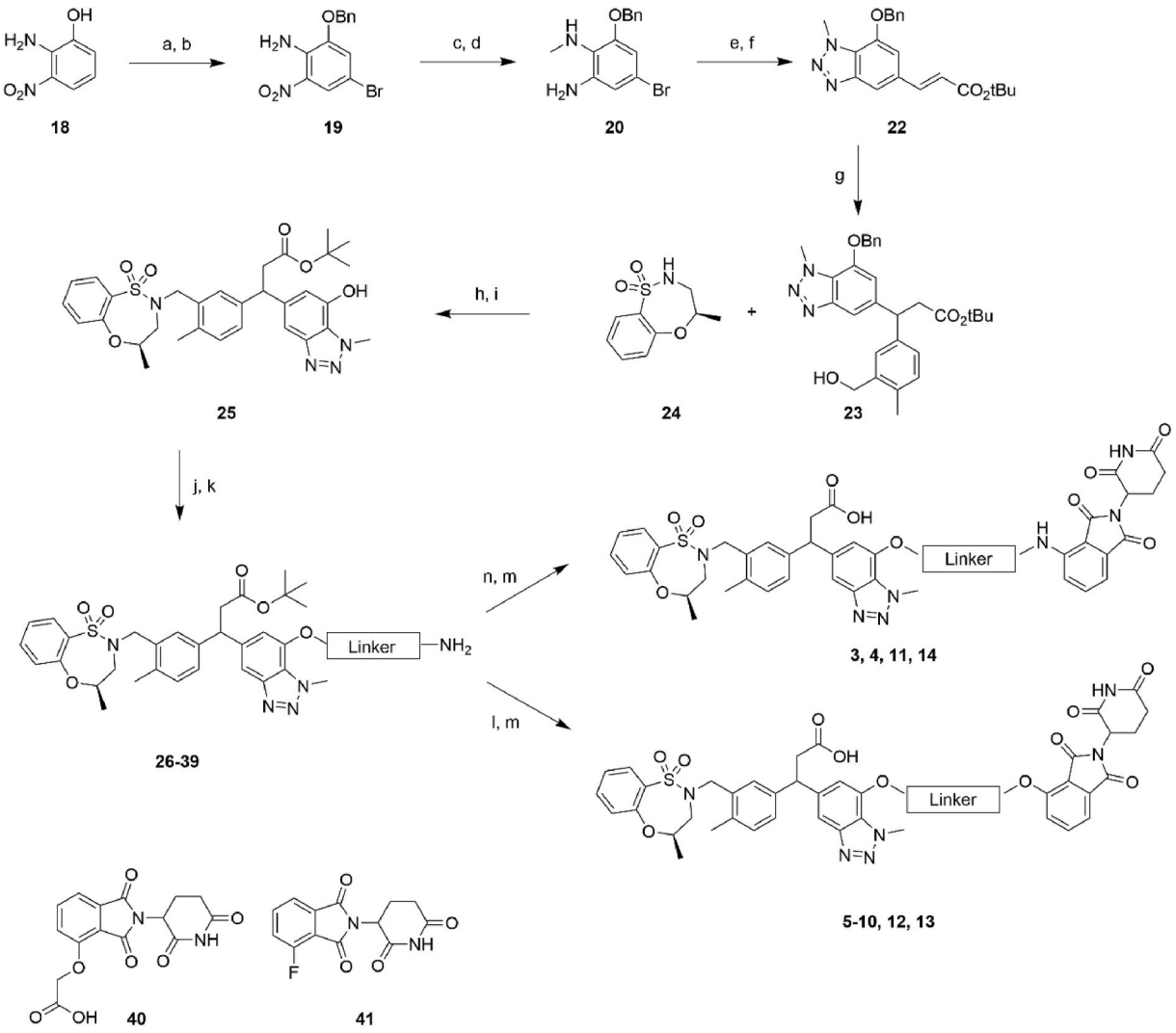

Scheme 1. General synthetic pathway to generate PROTACs. Reaction conditions: (a) K_2CO_3, BnBr, DMF, 0–20 °C; (b) AcOH, NaOAc, Br_2, 20 °C; (c) NaH, MeI, DMF, 0–20 °C; (d) Fe, AcOH, 65 °C; (e) $NaNO_2$, 10% aq. H_2SO_4; (f) *t*-butyl acrylate, DIPEA, P(*o*-tolyl)$_3$, $Pd(OAc)_2$, DMF, 95 °C; (g) $[RhCl(cod)]_2$, (3-(hydroxymethyl)-4-methylphenyl)boronic acid, Et_3N, dioxane, H_2O, 95 °C; (h) PPh_3, DIAD, THF, 0–20 °C; (i) Pd/C, H_2, MeOH, 20 °C; (j) K_2CO_3, alkyl halide, DMF, 80 °C; (k) Pd/C, H_2, MeOH; (l) **40**, HATU, DIPEA, DCM, 20 °C; (m) TFA, DCM, 20 °C; (n) **41**, DIPEA, DMF 80 °C.

Table 1
Activity of KEAP1 PROTACs against the KEAP1-Kelch domain.

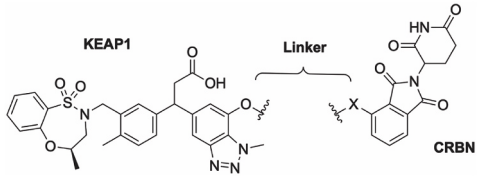

Cmpd	Linker	X	IC_{50} (SD) μM[a]
2	–	–	0.077 (0.003)
3		NH	0.150 (<0.001)
4		NH	0.267 (0.012)
5	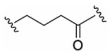	O	0.223 (0.006)
6	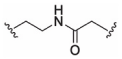	O	0.147 (0.006)
7	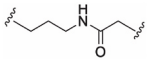	O	0.143 (0.012)
8	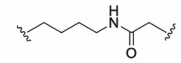	O	0.066 (0.006)
9	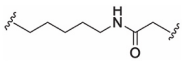	O	0.086 (0.002)
10	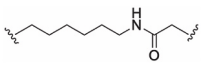	O	0.127 (0.006)
11	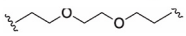	NH	0.120 (<0.001)
12	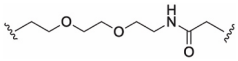	O	0.563 (0.029)
13	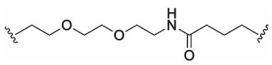	O	0.059 (0.001)

[a] IC_{50} (SD) values represent 3 independent experiments against recombinant KEAP1-Kelch domain in a HTRF biochemical assay.

at three lower concentrations (Fig. 2B and S2). PROTACs **8** (7-atom linker) and **10** (9-atom linker) were the most efficient at degrading KEAP1. Considering atom efficiency, we selected PROTAC **8** for further optimization.

Linker composition has been reported to affect the chemical stability of thalidomide-based PROTACs in cells [22]. While PROTAC **8** had the strongest effect on KEAP1 degradation at 24 h, it became less effective at longer time points of 48 h and 72 h, suggesting the stability of **8** was compromised in cells over time (Fig. 3 and S3). This data is consistent with previous reports that thalidomide-based heterobifunctional degraders conjugated via oxy-acetamide linkers are susceptible to hydrolysis in cells within 24 h [22]. To overcome instability, we synthesized PROTAC **14**, bearing a 7-atom linker and an amino-carbon linkage replacing the oxy-acetamide linkage to thalidomide (Fig. 3A and S3). PROTAC **14** had an IC_{50} of 46 nM in the KEAP1 HTRF biochemical assay, consistent with the activity of PROTAC **8** (IC_{50} 66 nM). A direct comparison of PROTACs **8** and **14** showed PROTAC **14** degraded KEAP1 more efficiently at 48 and 72 h compared to **8** (Fig. 3B and S3). At 24 h, PROTAC **14** also degraded KEAP1 more efficiently at lower concentrations than **8**. These data suggest the cellular stability of PROTAC **14** is enhanced, resulting in improved cellular degradation of KEAP1. Consequently, PROTAC **14** was selected for further characterization.

3.3. KEAP1 degradation mechanism of PROTAC *14*

The molecular mechanism underlying PROTAC **14**-mediated degradation of KEAP1 was verified in a competition experiment. HEK293T cells were pre-treated with the KEAP1 inhibitor **2** or thalidomide (TOM) to compete with PROTAC **14** for KEAP1 or CRBN binding, respectively. As shown in Fig. 4 and S4, KEAP1 degradation induced by **14** was significantly suppressed by the addition of excess **2** or thalidomide. These results demonstrate that simultaneous binding of PROTAC **14** to KEAP1 and CRBN is required for KEAP1 degradation. In addition, pre-treatment with the proteasome inhibitor MG132 prevented KEAP1 degradation, confirming degradation mediated by **14** was dependent on the cellular proteasomal machinery.

It is known that PROTACs can form unproductive binary complexes at excessive concentrations via saturated binding to the target protein or the E3 ligase, a phenomenon termed the hook effect [23]. To this extent, we evaluated PROTAC **14** in a dose titration experiment (0.01–8 μM) in HEK293T cells. A clear hook effect was observed with **14** at concentrations higher than 1 μM and where the maximum degradation (D_{max} = 94%) was observed (Fig. 4B and S5). The observed DC_{50} for KEAP1 in HEK293T cells was 11 nM (Fig. S5).

3.4. Activation of antioxidant response in cell lines induced by *14*

We next examined the ability of PROTAC **14** to activate the antioxidant response in different cell lines. In this study, we included compound **15** bearing an N-methylated glutarimide moiety, as a negative control for CRBN recruitment, and *tert*-butyl ester **16** as a negative control for KEAP1 binding, in addition to the covalent KEAP1 inhibitor sulforaphane (Sul). The KEAP1 inhibitor **2** was included as a benchmark positive control along with its negative control counterpart *tert*-butyl ester **17** (Fig. S6). HEK293T and HCA7 cell lines treated with PROTAC **14** for 48 h displayed robust degradation of KEAP1 which was not observed with other tested compounds. However, PROTAC **14** did not degrade KEAP1 in the lung cancer cell line A549, which harbors a G333C mutation in the KEAP1-Kelch domain [24] preventing the PROTAC **14** from binding (Fig. 5A and S7). Given that KEAP1 is the recruitment component of the Cullin3/Rbx1 E3 ligase complex, we assessed whether CRBN was able to be degraded by KEAP1 in these cell lines. Immunoblotting showed no change in CRBN levels upon treatment with PROTAC **14**, suggesting CRBN E3 ligase is outcompeting KEAP1 in this cellular system (Fig. 5A). In addition, changes in PROTAC linker length and composition (compounds **3**–**11**) did not affect CRBN levels in HEK293T cells (Fig. S8).

To measure the effect on antioxidant gene expression we monitored the protein levels of NRF2 downstream targets, NQO1 and HO-1 in the HEK293T and HCA7 cell lines following PROTAC **14** treatment. NQO1 and HO-1 were both upregulated by **14** in a dose-dependent manner, but to a lesser degree than observed with KEAP1 inhibitor **2** (Fig. 5A and S7). Compound **15** and sulforaphane upregulated NQO1, but not HO-1, expression. As expected, control compounds **16** and **17** showed no impact on KEAP1, NOQ1, or HO-1 expression.

To confirm the observed antioxidant response, PROTAC **14** was benchmarked against inhibitor **2** in a HepG2 cell line expressing an NRF2-responsive luciferase reporter, with an antioxidant response element (ARE) upstream of the firefly luciferase gene (Fig. 5B). PROTAC **14** treatment resulted in a dose-dependent increase in luciferase signal with a maximum 3.5-fold induction at 1 μM compared to the DMSO control group. In comparison, the KEAP1 inhibitor **2** showed a 5- to 6-fold increase in luciferase expression and was approximately 2-fold more potent than PROTAC **14**.

We next investigated the impact of KEAP1 degradation in BEAS-2B cells, a human non-tumorigenic lung epithelial cell line [25]. Notably, KEAP1 was more effectively degraded by PROTAC **14** in BEAS-2B cells with $DC_{50} < 1$ nM (Fig. 5A, S7, and S5), compared to KEAP1 degradation in HEK293T and HCA7 cell lines. Furthermore, PROTAC **14** was equipotent to KEAP1 inhibitor **2,** as evidenced by the increased expression of both NQO1 and GCLM at all tested concentrations (GCLM was measured in this cell line as HO-1 was not detectable by immunoblotting). The increased potency of PROTAC **14** in the BEAS-2B cell line could be due to the reduced basal levels of KEAP1 expression compared to HEK293T

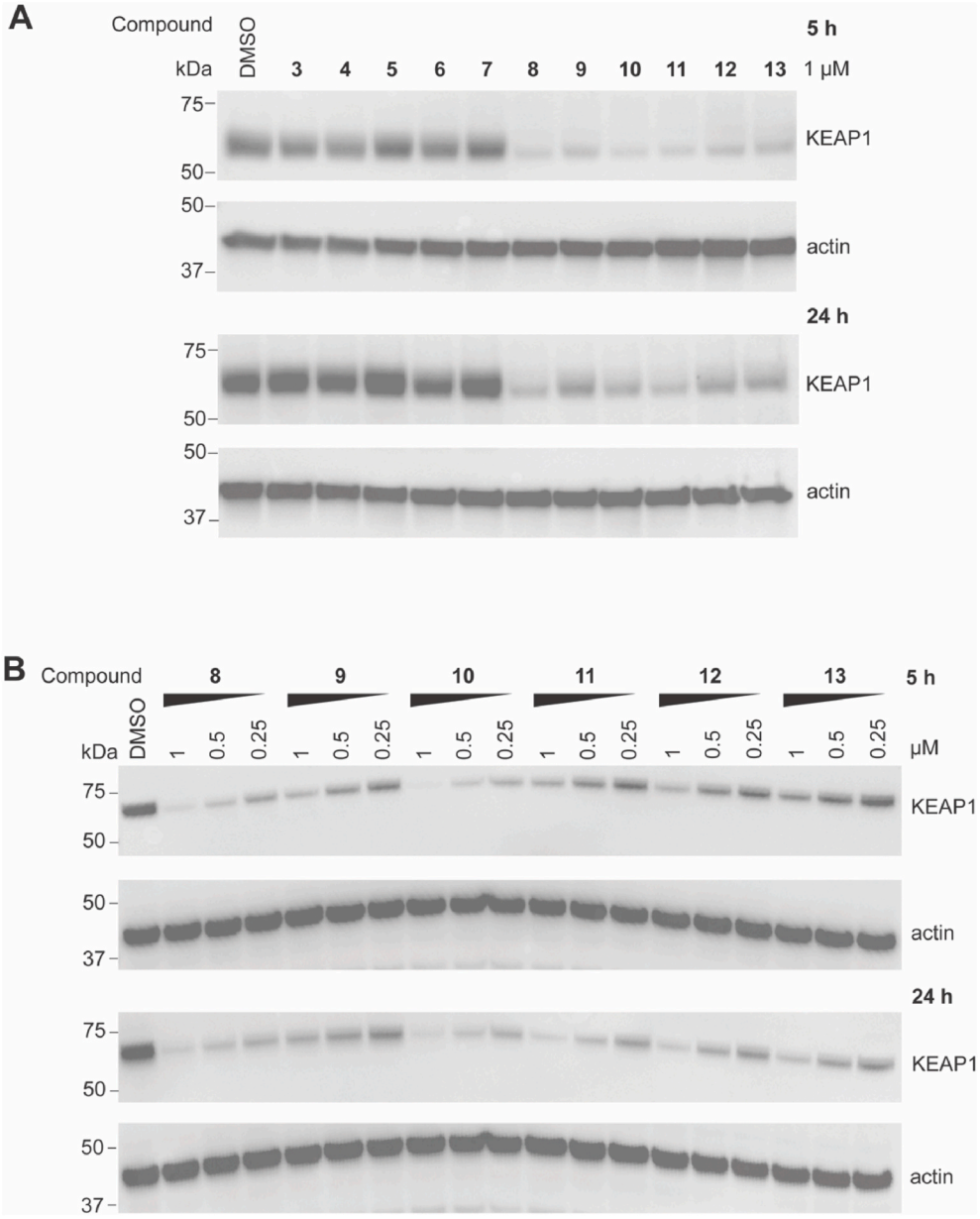

Fig. 2. Evaluation of PROTACs with different linkers on the degradation of KEAP1 in HEK293T cells. HEK293T cells were treated with DMSO vehicle control or 1 μM of compounds (**A**) at the indicated concentrations (**B**) for 5 and 24 h. Western blots are representative of 3 independent experiments. Repeats are shown in Figs. S1 and S2.

and HCA7 cell lines (Fig. S9).

To confirm the effect of PROTAC **14** on the expression of antioxidant genes, quantitative RT-PCR was employed to determine the mRNA levels of NQO1, TALDO1, and GCLM in the BEAS-2B cell line. 48 h treatment with PROTAC **14** or KEAP1 inhibitor **2** at 0.13 μM, resulted in similar levels of mRNA induction, with a 4-fold induction of NQO1 and a 2-fold induction of TALDO1 and GCLM (Fig. 5C). These findings highlight the antioxidant potential of PROTACs targeting KEAP1 for degradation in a lung epithelial model.

3.5. *Proteomics study of PROTAC **14***

Label-free quantitative proteomics was performed to identify the impact of KEAP1 degradation relative to KEAP1 inhibition in the BEAS-2B cell line. The proteomic results showed that PROTAC **14** significantly reduced the abundance of KEAP1, while other Kelch domain proteins such as KBTBD4, KLHDC2, and KLHL11 were not impacted, suggesting PROTAC **14** (and the inhibitor **2** from which it was derived) was highly selective for the KEAP1-Kelch domain (Fig. 6). PROTAC **14** significantly upregulated proteins commonly involved in the antioxidant response including GCLC, GCLM, SRXN1, ALDH3A1, PIR, TXNRD1, and ARK1C family proteins (Fig. 6A). Treatment with the KEAP1 inhibitor **2** did not affect KEAP1 expression and presented a similar pattern of antioxidant protein regulation, but some proteins although differentially expressed, did not achieve significance (Fig. 6B). Notably, NRF2 was not detected in the proteomic experiment, presumably due to its relative instability and short half-life [26].

PROTAC **14** was also found to regulate proteins involved in pathways not related to the antioxidant response (Fig. 6). For example, SQSTM1, another binding partner of KEAP1 [27], was upregulated on treatment with **14**. FTL and IREB2 proteins were other examples and participate in iron metabolism but have no known direct connection with the KEAP1-NRF2 signaling pathway [28]. ABHD4, a mitochondrial protein involved in lipid metabolism, was also significantly upregulated

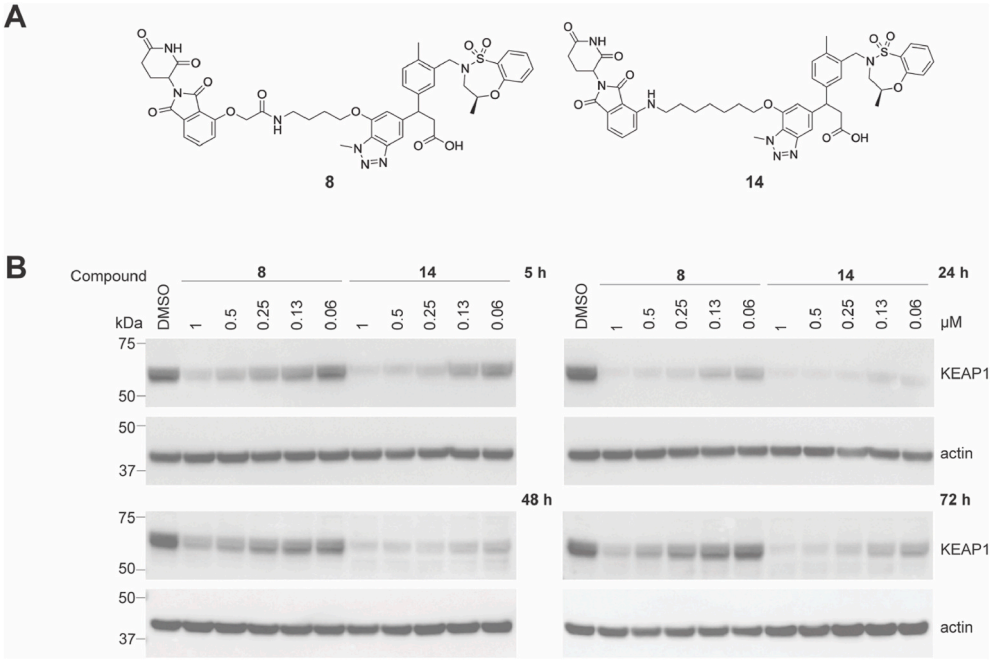

Fig. 3. A comparison of the KEAP1 degradation efficiency of compounds **8** and **14**. (**A**) Structures of compounds **8** and **14**. (**B**) HEK293T cells were treated with DMSO vehicle control or **8** and **14** at the indicated concentrations for 5, 24, 48, and 72 h. Immunoblots are representative of 3 independent experiments. Repeats are shown in Fig. S3.

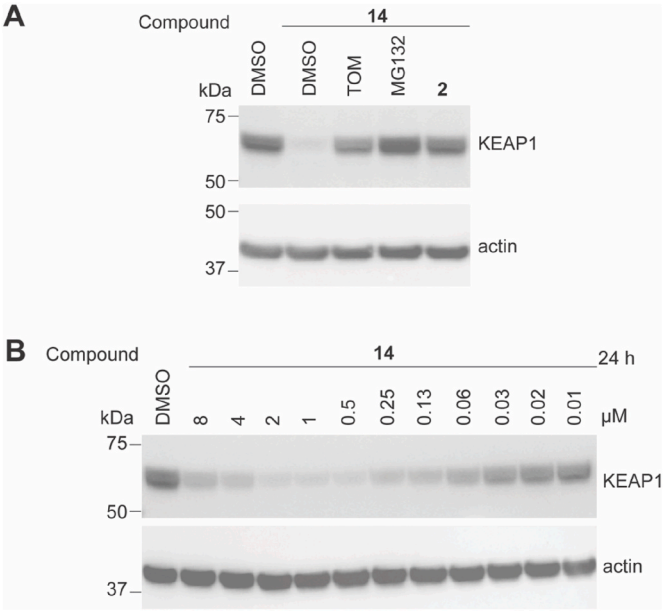

Fig. 4. Characterization of the targeted KEAP1 degradation capacity of compound **14**. (**A**) HEK293T cells were pre-treated with DMSO, 10 μM of thalidomide (TOM), 10 μM of proteasome inhibitor MG132, or 1 μM of inhibitor **2** for 1 h. Cells were then treated and incubated with **14** for 5 h. (**B**) HEK293T cells were treated with DMSO vehicle control or compound **14** at the indicated concentrations for 24 h. Immunoblots are representative of 3 independent repeats. Repeats are shown in Figs. S4 and S5.

by PROTAC **14**, whereas ABHD4 was not upregulated in BEAS-2B cells on treatment with inhibitor **2** (Fig. 6). ABHD4 is upregulated in NRF2 hyperactivated tumors [29], but the exact relationship with KEAP1 and the antioxidant pathway remains to be elucidated. Off-target degradation of ZFP91 induced by PROTAC **14** was also observed (Fig. 6A). ZFP91 is an established substrate of thalidomide-based immunomodulatory drugs (IMiDs) [30] and this observation is consistent with other previously reported CRBN-based PROTACs [31]. Levels of TK2, CALM1, TPD52L1, and PARP16 were also impacted by PROTAC **14** (Fig. 6A), but not the KEAP1 inhibitor **2** (Fig. 6B), possibly due to off-target degradation or an undefined connection with KEAP1-NRF2 signaling.

3.6. *Effects of anti-tBHP induced cell death by PROTAC **14** in BEAS-2B cells*

We next determined whether KEAP-1 degradation was sufficient to prevent ROS-induced cell death. *tert*-butyl hydroperoxide (tBHP) was chosen as the oxidative stress agent to impair BEAS-2B cell viability. BEAS-2B cells were pre-treated with PROTAC **14** or inhibitor **2** for 24 h and then exposed to 50 μM of tBHP for 24 h and cell viability was measured by flow cytometry (Fig. 7). PROTAC **14** and inhibitor **2** were equal potent between 500 and 16 nM but PROTAC **14** was less effective at concentrations lower than 16 nM, while the KEAP1 inhibitor **2** still maintained greater than 80% cell viability at similar concentrations. This data is consistent with the potent activation of the NRF antioxidant pathway observed for **2** and **14** (Fig. 5).

3.7. *PAMPA evaluation of PROTACs **8** and **14***

PROTACs typically have lower membrane permeability than the progenitor compounds on which they are designed [32–34]. Permeability is also a common issue encountered with the design of KEAP1 inhibitors [35,36] due to the requirement for a polar and ionizable carboxylic acid group that mimics the ETGE (and DLG) moiety of the NRF2 substrate [14]. To determine whether cell permeability is a contributing factor to the decreased cell activity of the KEAP1 PROTACs **8** and **14** compared to the KEAP1 inhibitor **2**, we performed a parallel artificial membrane permeability assay (PAMPA). The data shows that the KEAP1 inhibitor **2** and PROTACs **8** and **14** all have limited passive permeability in the PAMPA assay ($P_e < 0.005\ 10^{-6}$ cm/s) (Table S2). This suggests that passive cell permeability is not a contributing factor to the cell activity of the PROTACs **8** and **14** in comparison to the KEAP1

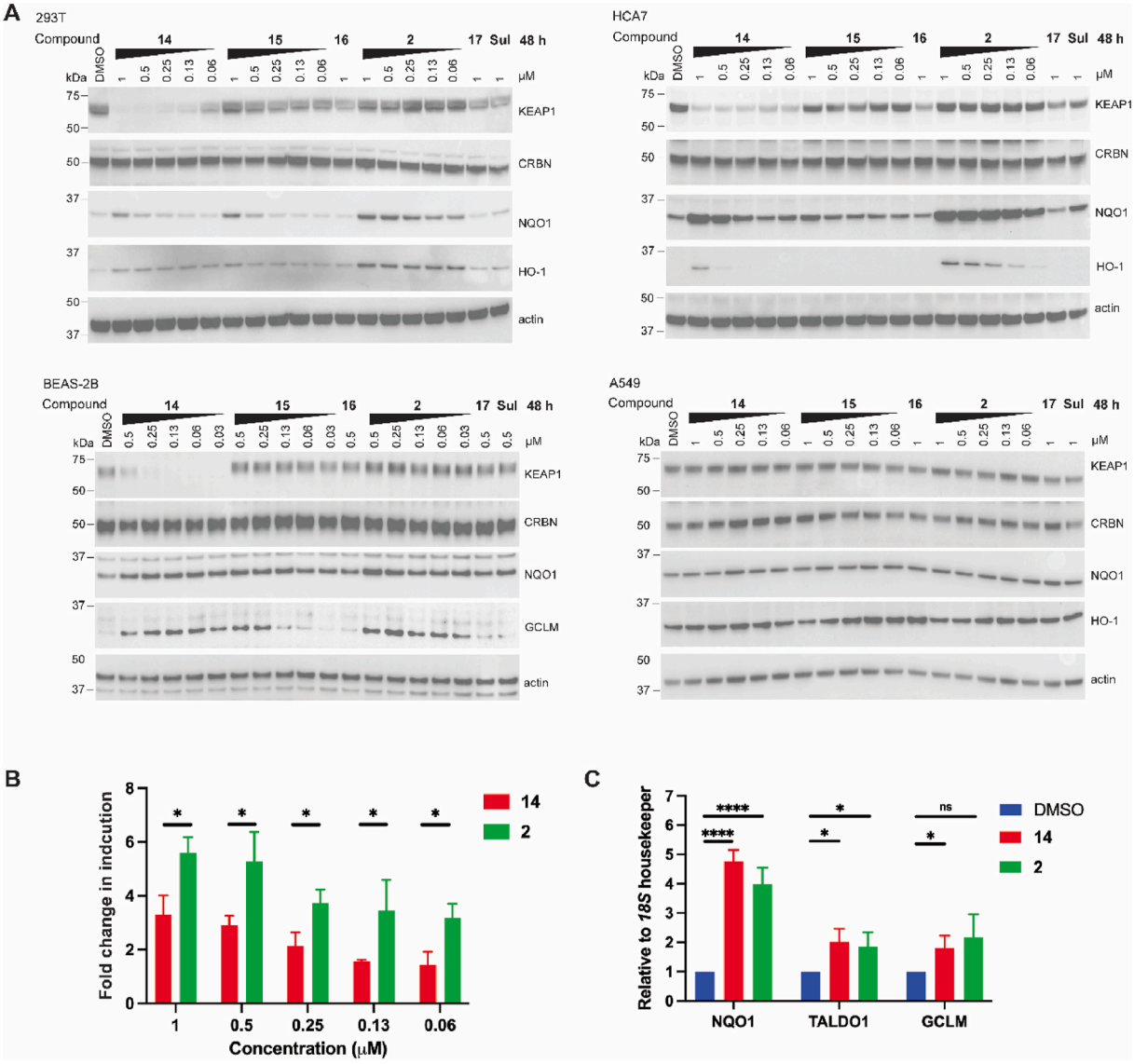

Fig. 5. Impact of PROTAC **14** on activation of the KEAP1/NRF2 signaling pathway. (**A**) HEK293T, HCA7, BEAS-2B, and A549 cells were treated with compounds at the indicated concentrations for 48 h. Immunoblots are representative of 3 independent experiments. Repeats are shown in Fig. S7. (**B**) HepG2 ARE-luciferase reporter cells were treated with compounds at the indicated concentrations for 48 h and luminescence was measured. Fold change in induction is relative to the DMSO control group. (**C**) BEAS-2B cells were treated with 0.13 μM of compounds for 48 h. The expression levels of the antioxidant signature genes were analyzed by RT-qPCR. For **B** and **C**, data shown are from three independent experiments, each of which was performed with technical triplicates. Data shown represent mean and S.D. Unpaired *t*-test was performed. (*) $p < 0.05$; (****) p 0.0001.

inhibitor **2**. The low permeability shown by all three compounds is somewhat surprising given the potent activity shown in cell assays (Sections 3.2 to 3.7). Active cell membrane transport mechanisms are not measured by PAMPA and therefore could be contributing to cell activity differences between the KEAP1 inhibitor **2** and PROTACs **8** and **14**.

4. Discussion

Inhibition of KEAP1 and subsequent activation of the NRF2 antioxidant response is an established and promising avenue to treat chronic diseases induced by oxidative stress. Currently, strategies are focused on the development of small molecules that either covalently interact with key cysteines on KEAP1 or directly disrupt the interaction between the KEAP1 Kelch domain and NRF2 [14]. In addition to traditional inhibitors, the PROTAC technology developed over the past two decades provides another strategy that not only inhibits but also deletes the target protein from cells [15]. At the time that this research was completed, Du et al. reported on a CRBN-based KEAP1 heterobifunctional degrader but did not investigate the consequence of KEAP1 depletion on the NRF2 antioxidant pathway in cell assays [37]. In our research, we synthesized and characterized a series of CRBN-based PROTACs targeting KEAP1 for proteasomal degradation and performed various assays to evaluate the effect of KEAP1 degradation on the NRF2 signaling axis. Through medicinal chemistry efforts and optimization of PROTAC linker type and length, a potent heterobifunctional degrader of KEAP1 (**14**) was identified. PROTAC **14** showed potent degradation of KEAP1 in HEK293T and BEAS-2B cell lines (DC_{50} 11 nM, D_{max} 94% @ 1 μM and $DC_{50} < 1$ nM, D_{max} 90% @ 62.5 nM, respectively) and was benchmarked against the parental inhibitor **2** in different cell lines comparing the activation of the NRF2 signaling pathway. In HEK293T and HCA7 cell lines, **14** effectively decreased KEAP1 protein levels, but NRF2 mediated gene expression was inferior compared to the KEAP1 inhibitor **2**. However, in the lung

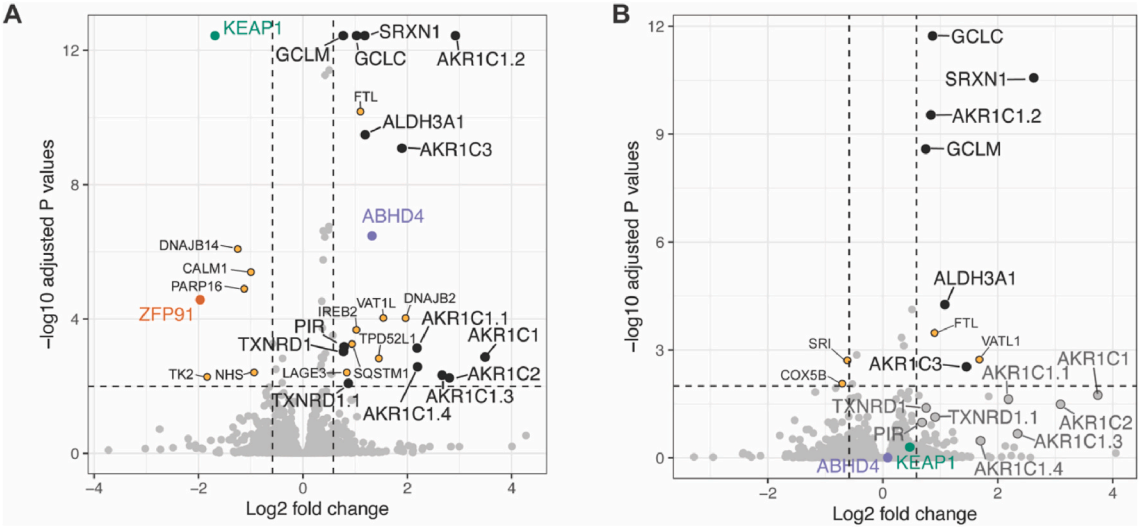

Fig. 6. KEAP1 degradation or inhibition induces anti-oxidant protein expression. Volcano plots showing differentially expressed proteins following treatment with **(A)** PROTAC **14**, and **(B)** inhibitor **2**. BEAS-2B cells were treated with DMSO, PROTAC **14**, or inhibitor **2** for 48 h, lysed and processed for proteomic analysis. Antioxidant proteins that were significantly changed following PROTAC **14** or inhibitor **2** treatment relative to the DMSO control, are highlighted as black dots (>1.5-fold abundance change and adjusted P value less than 0.01). Proteins that showed a significant change but were not directly related to antioxidant response are labeled with yellow dots. For **B**, antioxidant proteins that showed more than 1.5-fold change, but were not significant, are labeled as enlarged grey dots. KEAP1, ZFP91, and ABHD4 are labeled with green, orange, and purple colors, respectively. (For interpretation of the references to color in this figure legend, the reader is referred to the Web version of this article.)

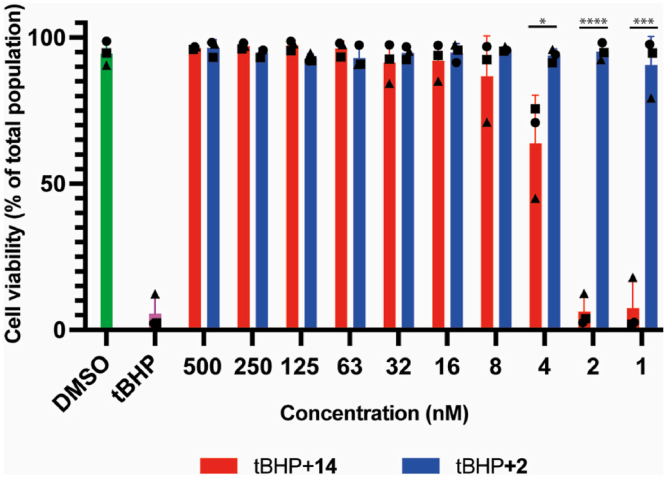

Fig. 7. KEAP1 degradation or inhibition rescues BEAS-2B cells from ROS induced cell death. BEAS-2B cells were pre-treated with the indicated compounds at various concentrations for 24 h and then exposed to 50 μM tBHP for an additional 24 h. Cells were harvested and the % of viable cells was analyzed by PI staining and flow cytometry. Data shown are from three independent assays, with each assay shown as a different symbol. Each assay was performed with single data points. Error bars represent average and S.D. Unpaired *t*-test was performed. (*) $p < 0.05$, (***) $p < 0.001$, (****) $p < 0.0001$.

epithelial BEAS-2B cells, PROTAC **14** induced NRF2 antioxidant gene expression to a similar level as the KEAP1 inhibitor **2**. The proteomics data confirmed that PROTAC **14** effectively reduced KEAP1 protein levels in cells and significantly increased the expression of proteins related to the NRF2 antioxidant response. Lastly, PROTAC **14** was shown to potently rescue BEAS-2B cells from ROS-induced cell death following treatment with tBHP comparable to **2**.

The PROTACs investigated were less potent binders to KEAP1 than the parent KEAP1 inhibitor **2**, as assessed via HTRF assay. In theory, PROTACs act by degrading the targeted protein via a catalytic mechanism, and therefore **14** would be expected to elicit equivalent or enhanced potency in activating the NRF2 antioxidant response compared to **2**. However, PROTAC **14** was consistently less effective than the KEAP1 inhibitor **2** in HEK239T and HCA7 cells. We show that the passive cellular permeability of the KEAP1 inhibitor **2** and the PROATCs **8** and **14** as measured by PAMPA (Table S2) was not contributing to the cell activity differences observed. Considering, the low passive cell membrane permeability, compound **2** and PROTACS **8** and **14** have remarkedly potent cell activity, and therefore it cannot be discounted that an active cell membrane transport mechanism (not measured by PAMPA) is contributing to cell activity and the differences observed with **14** (and **8**) in comparison to **2**. It is also possible that PROTAC **14** is degraded by cellular enzymes, however, compared to PROTAC **8** which has a cell stability liability, PROTAC **14** remains functional up to 72 h (Fig. 3). Furthermore, the formation of a ternary complex between PROTAC, E3 ligase, and the target protein is also a key factor in the observed degradative efficiency of a PROTAC. The ability of PROTAC **14** to induce an active ternary complex remains to be elucidated in further studies via SPR or X-ray crystallography and will be key to the future optimization of a KEAP1 targeted PROTAC.

We observed that PROTAC **14** was more potent in BEAS-2B cells compared to other cell lines. We rationalized that this could be due to the low basal expression level of KEAP1 in BEAS-2B cells (Fig. S9), which may not require a high intracellular concentration of **14** to induce NRF2 activation and potentially counterbalances the low cellular permeability and intracellular concentration of **14**. This observation highlights how the endogenous expression level of the target protein can impact the efficacy of a PROTAC.

KEAP1 forms a Cullin-Ring E3 ligase [11], and thus theoretically, may be able to degrade CRBN when both are recruited by the PROTAC. However, we did not observe CRBN degradation with our KEAP1-CRBN PROTACs (Fig. 5 and S8), suggesting that the CRBN E3 ligase complex was dominant over the KEAP1/Cul3/Rbx1 complex. This data is consistent with the results from Du et al. [37] showing KEAP1 is degraded by both KEAP1-CRBN and KEAP1-VHL PROTACs. Interestingly, the opposite was found for a CRBN-VHL PROTAC which degraded CRBN and not VHL [38–41], while the MDM2-CRBN PROTAC degraded MDM2 [42]. It is unknown why CRBN and VHL E3 ligases dominate over KEAP1, but KEAP1 was shown to have a modest degradative capacity as

the E3 component in a PROTAC to degrade bromodomain and focal adhesion kinase proteins [21,37]. It is postulated that KEAP1 dimerization is required to achieve optimal degradative capacity, as seen with ubiquitination of the native KEAP1 substrate NRF2, with the PROTAC or ternary PROTAC complex needing to engage with both juxtaposed KEAP1-kelch molecules in the homodimeric degradative E3 complex [8,9]. Above all, further optimization of the linker to form an active ternary complex may be required to fully harness the E3 degradative ability of KEAP1 in a PROTAC strategy.

As proof-of-principle, we have demonstrated that PROTAC **14** can efficiently degrade KEAP1 in cells, however, further optimization is required to enhance cell permeability, target selectivity, and pharmacological properties such as metabolism that are an important considerations for efficacy in animal models. The optimization may include rigidifying the linker by introducing heterocyclic scaffolds such as piperazine and piperidines, a strategy that has been used previously to improve cell membrane permeability [43,44]. Carboxylic acid isosteres or a prodrug approach previously applied to KEAP1 inhibitors [35,36] could also be introduced to mask the polar carboxylic acid group to improve cell membrane permeability. Although the stability of the CRBN ligand was improved in our study, the thalidomide ligand could be replaced by other phenyl glutarimide analogs which have been reported to have greater metabolic stability [45]. To overcome undesirable off-target consequences of the CRBN ligand, recruitment of the VHL E3 ligase could be considered in the design of a KEAP1 heterobifunctional degrader [46]. Du et al. have shown that VHL-based PROTAC at high concentrations can degrade KEAP1 [37], proving a VHL-based concept but also suggesting further optimization is required. The incorporation of a VHL ligand may also favor the formation of an active ternary complex between the E3 ligase and KEAP1 to improve degradative efficiency. The switch to a VHL ligand will also enable optimization to be guided by biophysical and structural data [43], whereas this is challenging with CRBN because of the technical difficulties we experienced with the expression of recombinant CRBN constructs.

In conclusion, the KEAP1 targeted PROTAC designed here is a useful tool for studying the biological consequences of KEAP1 degradation. This work established the possibility of degrading KEAP1 as an alternative to existing KEAP1 therapeutic strategies that covalently or directly inhibit KEAP1. Further development of the KEAP1 bifunctional degrader is required to fully understand the implications of KEAP1 degradation *in vitro* and in animal models, working toward a new treatment for oxidative stress-induced disorders.

Conflict of interest

All authors have approved the final version of the manuscript and declare no conflict of interest related to this work.

Declaration of competing interest

All authors have approved the final version of the manuscript and declare no conflict of interest related to this work.

Data availability

Data will be made available on request.

Acknowledgments

This work was supported by the Australian Cancer Research Foundation and the Victorian State Government Operational Infrastructure Support and Australian Government NHMRC IRIISS. The laboratory of R.F. is supported by The Galbraith Family Charitable Trust and the K & M Foundation for Women. R.F. and B.C.L received grant funding from the Australian Government via the MRFF Frontier program (Grant ID: RFRHPI000269). B.E.S. is a Corin Centenary Fellow. G.B. is supported by an Australian Government Research Training Program scholarship and H.C. is supported by a Research Scholarship from the University of Melbourne.

Appendix A. Supplementary data

Supplementary data to this article can be found online at https://doi.org/10.1016/j.redox.2022.102552.

Abbreviations

ABHD4	Alpha/beta-hydrolase domain containing 4
ALDH3A1	Aldehyde dehydrogenase 3A1
ARE	Antioxidant response element
ARK1C	Aldo/keto reductase family1 member C1
BSA	Bovine serum albumin
BTB	Broad complex, tramtrack and bric-à-brac
CALM1	Calmodulin 1
CRBN	Cereblon
E3	Ubiquitin ligase
FACS	Fluorescence-activated cell sorting
FTL	Ferritin light chain
GCLM	Glutamate-cysteine ligase modifier subunit
HEPES	4-(2-hydroxyethyl)-1-piperazineethanesulfonic acid
HO-1	Heme oxygenase-1
HRP	Horse radish peroxidase
IMiDs	Immunomodulatory drugs
IREB2	Iron responsive element binding protein 2
IVR	Intervening region
KBTBD4	Kelch repeat and BTB domain containing 4
KEAP1	Kelch-like ECH-associated protein 1
KLHDC2	Kelch domain containing 2
KLHL11	Kelch like family member 11
NQO1	NAD(P)H:quinone oxidoreductase 1
NRF2	Nuclear factor erythroid 2–related factor 2
PAMPA	Parallel artificial membrane permeability assay
PARP16	Poly (ADP-ribose) polymerase family member 16
PI	Propidium iodide
PIR	Pirin
POI	Protein of interest
PROTAC	Proteolysis-targeting chimeras
RBX1	RING-box protein 1
RING	Really interesting new gene
ROS	Reactive oxygen species
SQSTM1	Sequestosome 1
SRXN1	Sulfiredoxin 1
TALDO1	Transaldolase 1
tBHP	*tert*-butyl hydroperoxide
TK2	Thymidine kinase 2
TOM	Thalidomide
TPD52L1	Tumor protein D52 like 1
TXNRD1	Thioredoxin reductase 1
UPS	Ubiquitin–proteasome system
VHL	Hippel–Lindau tumour suppressor
ZFP91	Zinc finger protein 91

References

[1] H. Sies, Oxidative stress: a concept in redox biology and medicine, Redox Biol. 4 (2015) 180–183.
[2] G. Pizzino, N. Irrera, M. Cucinotta, G. Pallio, F. Mannino, V. Arcoraci, F. Squadrito, D. Altavilla, A. Bitto, Oxidative stress: harms and benefits for human health, Oxid. Med. Cell. Longev. 2017 (2017), 8416763.
[3] L. He, T. He, S. Farrar, L. Ji, T. Liu, X. Ma, Antioxidants maintain cellular redox homeostasis by elimination of reactive oxygen species, Cell. Physiol. Biochem. 44 (2) (2017) 532–553.

[4] S. Dayalan Naidu, A.T. Dinkova-Kostova, KEAP1, a cysteine-based sensor and a drug target for the prevention and treatment of chronic disease, Open Biol 10 (6) (2020), 200105.

[5] N. Wakabayashi, A.T. Dinkova-Kostova, W.D. Holtzclaw, M.I. Kang, A. Kobayashi, M. Yamamoto, T.W. Kensler, P. Talalay, Protection against electrophile and oxidant stress by induction of the phase 2 response: fate of cysteines of the Keap1 sensor modified by inducers, Proc. Natl. Acad. Sci. U. S. A. 101 (7) (2004) 2040–2045.

[6] O. Albagli, P. Dhordain, C. Deweindt, G. Lecocq, D. Leprince, The BTB/POZ domain: a new protein-protein interaction motif common to DNA- and actin-binding proteins, Cell Growth Differ. 6 (9) (1995) 1193–1198.

[7] A. Cleasby, J. Yon, P.J. Day, C. Richardson, I.J. Tickle, P.A. Williams, J.F. Callahan, R. Carr, N. Concha, J.K. Kerns, H. Qi, T. Sweitzer, P. Ward, T.G. Davies, Structure of the BTB domain of Keap1 and its interaction with the triterpenoid antagonist CDDO, PLoS One 9 (6) (2014), e98896.

[8] P. Canning, C.D.O. Cooper, T. Krojer, J.W. Murray, A.C.W. Pike, A. Chaikuad, T. Keates, C. Thangaratnarajah, V. Hojzan, B.D. Marsden, O. Gileadi, S. Knapp, F. von Delft, A.N. Bullock, Structural basis for Cul3 protein assembly with the BTB-Kelch family of E3 ubiquitin ligases, J. Biol. Chem. 288 (11) (2013) 7803–7814.

[9] P. Canning, F.J. Sorrell, A.N. Bullock, Structural basis of Keap1 interactions with Nrf2, Free Radic. Biol. Med. 88 (Pt B) (2015) 101–107.

[10] K.I. Tong, Y. Katoh, H. Kusunoki, K. Itoh, T. Tanaka, M. Yamamoto, Keap1 recruits Neh2 through binding to ETGE and DLG motifs: characterization of the two-site molecular recognition model, Mol. Cell Biol. 26 (8) (2006) 2887–2900.

[11] A. Kobayashi, M.I. Kang, H. Okawa, M. Ohtsuji, Y. Zenke, T. Chiba, K. Igarashi, M. Yamamoto, Oxidative stress sensor Keap1 functions as an adaptor for Cul3-based E3 ligase to regulate proteasomal degradation of Nrf2, Mol. Cell Biol. 24 (16) (2004) 7130–7139.

[12] L. Baird, M. Yamamoto, The molecular mechanisms regulating the KEAP1-NRF2 pathway, Mol. Cell Biol. 40 (13) (2020) e00099-20.

[13] A. Cuadrado, A.I. Rojo, G. Wells, J.D. Hayes, S.P. Cousin, W.L. Rumsey, O. C. Attucks, S. Franklin, A.L. Levonen, T.W. Kensler, A.T. Dinkova-Kostova, Therapeutic targeting of the NRF2 and KEAP1 partnership in chronic diseases, Nat. Rev. Drug Discov. 18 (4) (2019) 295–317.

[14] H. Zhou, Y. Wang, Q. You, Z. Jiang, Recent progress in the development of small molecule Nrf2 activators: a patent review (2017-present), Expert Opin. Ther. Pat. 30 (3) (2020) 209–225.

[15] A.C. Lai, C.M. Crews, Induced protein degradation: an emerging drug discovery paradigm, Nat. Rev. Drug Discov. 16 (2) (2017) 101–114.

[16] Y. Zou, D. Ma, Y. Wang, The PROTAC technology in drug development, Cell Biochem. Funct. 37 (1) (2019) 21–30.

[17] P. Ottis, C.M. Crews, Proteolysis-targeting chimeras: induced protein degradation as a therapeutic strategy, ACS Chem. Biol. 12 (4) (2017) 892–898.

[18] H. Chen, Y. Wu, K. Li, I. Currie, N. Keating, F. Dehkhoda, C. Grohmann, J.J. Babon, S.E. Nicholson, B.E. Sleebs, Optimization of phosphotyrosine peptides that target the SH2 domain of SOCS1 and block substrate ubiquitination, ACS Chem. Biol. 17 (2) (2022) 449–462.

[19] H. Chen, T.M.B. Ware, J. Iaria, H.J. Zhu, Live cell imaging of the TGF- beta/smad3 signaling pathway in vitro and in vivo using an adenovirus reporter system, JoVE 137 (2018).

[20] T.G. Davies, W.E. Wixted, J.E. Coyle, C. Griffiths-Jones, K. Hearn, R. McMenamin, D. Norton, S.J. Rich, C. Richardson, G. Saxty, H.M. Willems, A.J. Woolford, J. E. Cottom, J.P. Kou, J.G. Yonchuk, H.G. Feldser, Y. Sanchez, J.P. Foley, B. J. Bolognese, G. Logan, P.L. Podolin, H. Yan, J.F. Callahan, T.D. Heightman, J. K. Kerns, Monoacidic inhibitors of the Kelch-like ECH-associated protein 1: nuclear factor erythroid 2-related factor 2 (KEAP1:NRF2) protein-protein interaction with high cell potency identified by fragment-based discovery, J. Med. Chem. 59 (8) (2016) 3991–4006.

[21] J. Wei, F. Meng, K.S. Park, H. Yim, J. Velez, P. Kumar, L. Wang, L. Xie, H. Chen, Y. Shen, E. Teichman, D. Li, G.G. Wang, X. Chen, H.U. Kaniskan, J. Jin, Harnessing the E3 ligase KEAP1 for targeted protein degradation, J. Am. Chem. Soc. 143 (37) (2021) 15073–15083.

[22] A. Bricelj, Y.L. Dora Ng, D. Ferber, R. Kuchta, S. Muller, M. Monschke, K. G. Wagner, J. Kronke, I. Sosic, M. Gutschow, C. Steinebach, Influence of linker attachment points on the stability and neosubstrate degradation of cereblon ligands, ACS Med. Chem. Lett. 12 (11) (2021) 1733–1738.

[23] K. Moreau, M. Coen, A.X. Zhang, F. Pachl, M.P. Castaldi, G. Dahl, H. Boyd, C. Scott, P. Newham, Proteolysis-targeting chimeras in drug development: a safety perspective, Br. J. Pharmacol. 177 (8) (2020) 1709–1718.

[24] A. Singh, V. Misra, R.K. Thimmulappa, H. Lee, S. Ames, M.O. Hoque, J.G. Herman, S.B. Baylin, D. Sidransky, E. Gabrielson, M.V. Brock, S. Biswal, Dysfunctional KEAP1-NRF2 interaction in non-small-cell lung cancer, PLoS Med. 3 (10) (2006), e420.

[25] R.R. Reddel, Y. Ke, B.I. Gerwin, M.G. McMenamin, J.F. Lechner, R.T. Su, D. E. Brash, J.B. Park, J.S. Rhim, C.C. Harris, Transformation of human bronchial epithelial cells by infection with SV40 or adenovirus-12 SV40 hybrid virus, or transfection via strontium phosphate coprecipitation with a plasmid containing SV40 early region genes, Cancer Res. 48 (7) (1988) 1904–1909.

[26] F. He, X. Ru, T. Wen, NRF2, a transcription factor for stress response and beyond, Int. J. Mol. Sci. 21 (13) (2020).

[27] M. Komatsu, H. Kurokawa, S. Waguri, K. Taguchi, A. Kobayashi, Y. Ichimura, Y. S. Sou, I. Ueno, A. Sakamoto, K.I. Tong, M. Kim, Y. Nishito, S. Iemura, T. Natsume, T. Ueno, E. Kominami, H. Motohashi, K. Tanaka, M. Yamamoto, The selective autophagy substrate p62 activates the stress responsive transcription factor Nrf2 through inactivation of Keap1, Nat. Cell Biol. 12 (3) (2010) 213–223.

[28] X. Chen, C. Yu, R. Kang, D. Tang, Iron metabolism in ferroptosis, Front. Cell Dev. Biol. 8 (2020), 590226.

[29] S.E. Lacher, M. Slattery, Gene regulatory effects of disease-associated variation in the NRF2 network, Curr Opin Toxicol 1 (2016) 71–79.

[30] J. An, C.M. Ponthier, R. Sack, J. Seebacher, M.B. Stadler, K.A. Donovan, E. S. Fischer, pSILAC mass spectrometry reveals ZFP91 as IMiD-dependent substrate of the CRL4(CRBN) ubiquitin ligase, Nat. Commun. 8 (2017), 15398.

[31] D.P. Bondeson, B.E. Smith, G.M. Burslem, A.D. Buhimschi, J. Hines, S. Jaime-Figueroa, J. Wang, B.D. Hamman, A. Ishchenko, C.M. Crews, Lessons in PROTAC design from selective degradation with a promiscuous warhead, Cell Chem. Biol. 25 (1) (2018) 78–87 e5.

[32] C. Cecchini, S. Pannilunghi, S. Tardy, L. Scapozza, From conception to development: investigating PROTACs features for improved cell permeability and successful protein degradation, Front. Chem. 9 (2021), 672267.

[33] C.A. Foley, F. Potjewyd, K.N. Lamb, L.I. James, S.V. Frye, Assessing the cell permeability of bivalent chemical degraders using the chloroalkane penetration assay, ACS Chem. Biol. 15 (1) (2020) 290–295.

[34] D.E. Scott, T.P.C. Rooney, E.D. Bayle, T. Mirza, H.M.G. Willems, J.H. Clarke, S. P. Andrews, J. Skidmore, Systematic investigation of the permeability of androgen receptor PROTACs, ACS Med. Chem. Lett. 11 (8) (2020) 1539–1547.

[35] M. Lu, X. Zhang, J. Zhao, Q. You, Z. Jiang, A hydrogen peroxide responsive prodrug of Keap1-Nrf2 inhibitor for improving oral absorption and selective activation in inflammatory conditions, Redox Biol. 34 (2020), 101565.

[36] J.S. Pallesen, D. Narayanan, K.T. Tran, S.M.Ø. Solbak, G. Marseglia, L.M. E. Sørensen, L.J. Høj, F. Munafò, R.M.C. Carmona, A.D. Garcia, H.L. Desu, R. Brambilla, T.N. Johansen, G.M. Popowicz, M. Sattler, M. Gajhede, A. Bach, Deconstructing noncovalent kelch-like ECH-associated protein 1 (Keap1) inhibitors into fragments to reconstruct new potent compounds, J. Med. Chem. 64 (8) (2021) 4623–4661.

[37] G. Du, J. Jiang, N.J. Henning, N. Safaee, E. Koide, R.P. Nowak, K.A. Donovan, H. Yoon, I. You, H. Yue, N.A. Eleuteri, Z. He, Z. Li, H.T. Huang, J. Che, B. Nabet, T. Zhang, E.S. Fischer, N.S. Gray, Exploring the target scope of KEAP1 E3 ligase-based PROTACs, Cell Chem Biol 29 (10) (2022) 1470–1481.

[38] M. Girardini, C. Maniaci, S.J. Hughes, A. Testa, A. Ciulli, Cereblon versus VHL: hijacking E3 ligases against each other using PROTACs, Bioorg. Med. Chem. 27 (12) (2019) 2466–2479.

[39] K. Kim, D.H. Lee, S. Park, S.H. Jo, B. Ku, S.G. Park, B.C. Park, Y.U. Jeon, S. Ahn, C. H. Kang, D. Hwang, S. Chae, J.D. Ha, S. Kim, J.Y. Hwang, J.H. Kim, Disordered region of cereblon is required for efficient degradation by proteolysis-targeting chimera, Sci. Rep. 9 (1) (2019), 19654.

[40] C.E. Powell, G. Du, J.W. Bushman, Z. He, T. Zhang, E.S. Fischer, N.S. Gray, Selective degradation-inducing probes for studying cereblon (CRBN) biology, RSC Med Chem 12 (8) (2021) 1381–1390.

[41] C. Steinebach, H. Kehm, S. Lindner, L.P. Vu, S. Köpff, Á. López Mármol, C. Weiler, K.G. Wagner, M. Reichenzeller, J. Krönke, M. Gütschow, PROTAC-mediated crosstalk between E3 ligases, Chem. Commun. 55 (12) (2019) 1821–1824.

[42] Y. Li, J. Yang, A. Aguilar, D. McEachern, S. Przybranowski, L. Liu, C.-Y. Yang, M. Wang, X. Han, S. Wang, Discovery of MD-224 as a first-in-class, highly potent, and efficacious proteolysis targeting chimera murine double minute 2 degrader capable of achieving complete and durable tumor regression, J. Med. Chem. 62 (2) (2019) 448–466.

[43] W. Farnaby, M. Koegl, M.J. Roy, C. Whitworth, E. Diers, N. Trainor, D. Zollman, S. Steurer, J. Karolyi-Oezguer, C. Riedmueller, T. Gmaschitz, J. Wachter, C. Dank, M. Galant, B. Sharps, K. Rumpel, E. Traxler, T. Gerstberger, R. Schnitzer, O. Petermann, P. Greb, H. Weinstabl, G. Bader, A. Zoephel, A. Weiss-Puxbaum, K. Ehrenhofer-Wolfer, S. Wohrle, G. Boehmelt, J. Rinnenthal, H. Arnhof, N. Wiechens, M.Y. Wu, T. Owen-Hughes, P. Ettmayer, M. Pearson, D.B. McConnell, A. Ciulli, BAF complex vulnerabilities in cancer demonstrated via structure-based PROTAC design, Nat. Chem. Biol. 15 (7) (2019) 672–680.

[44] X. Han, C. Wang, C. Qin, W. Xiang, E. Fernandez-Salas, C.Y. Yang, M. Wang, L. Zhao, T. Xu, K. Chinnaswamy, J. Delproposto, J. Stuckey, S. Wang, Discovery of ARD-69 as a highly potent proteolysis targeting chimera (PROTAC) degrader of androgen receptor (AR) for the treatment of prostate cancer, J. Med. Chem. 62 (2) (2019) 941–964.

[45] J. Min, A. Mayasundari, F. Keramatnia, B. Jonchere, S.W. Yang, J. Jarusiewicz, M. Actis, S. Das, B. Young, J. Slavish, L. Yang, Y. Li, X. Fu, S.H. Garrett, M.K. Yun, Z. Li, S. Nithianantham, S. Chai, T. Chen, A. Shelat, R.E. Lee, G. Nishiguchi, S. W. White, M.F. Roussel, P.R. Potts, M. Fischer, Z. Rankovic, Phenyl-glutarimides: alternative cereblon binders for the design of PROTACs, Angew Chem. Int. Ed. Engl. 60 (51) (2021) 26663–26670.

[46] C.J. Diehl, A. Ciulli, Discovery of small molecule ligands for the von Hippel-Lindau (VHL) E3 ligase and their use as inhibitors and PROTAC degraders, Chem. Soc. Rev. 51 (2022) 8216–8257.